Regional brain activity of resting-state fMRI and auditory oddball ERP with multimodal approach in individuals with internet gaming disorder

MINKYUNG PARK[1] , JOON HWAN JANG[2,3] ,
SO YOUNG YOO[4] , AREUM CHOI[1] ,
HEEJUNG KIM[5,6]** and JUNG-SEOK CHOI[1]*

[1] Department of Psychiatry, Samsung Medical Center, Sungkyunkwan University School of Medicine, Seoul, Republic of Korea

[2] Department of Psychiatry, Seoul National University Health Service Center, Seoul, Republic of Korea

[3] Department of Human Systems Medicine, Seoul National University College of Medicine, Seoul, Republic of Korea

[4] Department of Psychiatry, SMG-SNU Boramae Medical Center, Seoul, Republic of Korea

[5] Department of Nuclear Medicine, SMG-SNU Boramae Medical Center, Seoul, Republic of Korea

[6] Institute of Radiation Medicine, Medical Research Center, Seoul National University, Seoul, Republic of Korea

ABSTRACT

Background and aims: Resting-state brain activity may be associated with the ability to perform tasks; however, a multimodal approach involving resting-state functional magnetic resonance imaging (fMRI) and event-related potentials (ERPs) has not been widely used to investigate addictive disorders. *Methods:* We explored resting-state fMRI and auditory oddball ERP values from 26 with internet gaming disorder (IGD) patients and 27 age- and intelligence quotient-matched healthy controls (HCs). To assess the characteristics of resting-state fMRI, we calculated regional homogeneity (ReHo), amplitude of low-frequency fluctuation (ALFF), and fractional amplitude of low-frequency fluctuation (fALFF); we also calculated the P3 component of the ERPs. *Results:* Compared with HCs, the individuals with IGD exhibited significant decreases in ReHo and fALFF values in the left inferior occipital gyrus, increased ReHo and ALFF values in the right precuneus, increased ALFF in the left superior frontal gyrus, and lower P3 amplitudes in the midline centro-parietal area during the auditory ERP task. Furthermore, the regional activity of resting-state fMRI in the right inferior temporal gyrus and the occipital regions were positively correlated with the P3 amplitudes in IGD patients, whereas ReHo values of the left hippocampus and the right amygdala were negatively correlated with P3. *Discussion and conclusions:* Our results suggest that IGD patients have difficulty interacting effectively with cognitive function and sensory processing, although its interpretations need some cautions. The findings in this study will broaden the overall understanding of the neurobiological mechanisms that underlie IGD pathophysiology.

*Corresponding author.
E-mail: choijs73@gmail.com

**Corresponding author.
E-mail: hjkim72@snu.ac.kr

INTRODUCTION

A balance between top-down and bottom-up strategies is needed to maintain mental health and well-being. Internet gaming disorder (IGD) is a mental health condition defined by the

loss of control over internet gaming and repeated use of internet games; IGD has been included as a gaming disorder in the 11th revision of the International Classification of Diseases (ICD-11). Although proper internet gaming activities can help to alleviate loneliness and stress, excessive gaming can have adverse consequences on mental health (Mestre-Bach, Granero, Fernández-Aranda, Jiménez-Murcia, & Potenza, 2023; Park et al., 2021).

Many neuroimaging and neurophysiology studies have investigated the features of human brain function. Advanced functional magnetic resonance imaging (fMRI) has high spatial resolution but low time resolution (i.e., hundreds of milliseconds). EEG has excellent time resolution (i.e., milliseconds) but its spatial resolution is limited because of head volume conduction (Nunez et al., 1997). Therefore, fMRI and EEG are complementary neuroimaging techniques. The integration of fMRI and EEG may be useful for exploring neural correlates between fMRI and EEG features; it may also help to integrate neural brain activities from different perspectives.

Resting-state fMRI studies have revealed alterations in various aspects of brain function among patients with IGD. Regional homogeneity (ReHo), amplitude of low-frequency fluctuation (ALFF), and fractional amplitude of low-frequency fluctuation (fALFF) have been used to investigate the regional characteristics of resting-state fMRI signals (Zou et al., 2008). ReHo assumes that the regional blood oxygen level-dependent (BOLD) signal within a particular voxel is temporally similar to the signals of its neighbors and could be modulated in related cognitive tasks (Zang, Jiang, Lu, He, & Tian, 2004). ALFF and fALFF are used to characterize the regional intensity of brain activity by indexing low-frequency fluctuations in spontaneous neuronal activity (Yu-Feng et al., 2007). ALFF is sensitive to physiological noise but may also be sensitive to pathological changes. fALFF is a mathematical method for suppressing physiological noise (Zou et al., 2008). Therefore, analyses using ReHo, ALFF, and fALFF provide a more comprehensive understanding of the neural bases of the brain during the exploration of regional activity in resting-state fMRI. Abnormalities in ReHo, ALFF, and fALFF may be associated with dysfunction in regional brain activity and have been identified in patients with various neurological and psychiatric disorders (Han et al., 2011; Hoptman et al., 2010).

Previous studies have shown that IGD patients exhibit enhanced ReHo in brain regions involved in sensory-motor coordination and decreased ReHo in brain regions responsible for visual and auditory functions (Dong, Huang, & Du, 2012). Compared with healthy controls (HCs), IGD patients have increased ReHo values in the posterior cingulate cortex; moreover, changes in ReHo in the precuneus/posterior cingulate cortex are associated with the severity of IGD symptoms in the individuals with IGD (Kim et al., 2015). Changes in ALFF have been reported in the left orbitofrontal cortex, the left precuneus, and the left supplementary motor cortex in IGD patients (Yuan, Jin, et al., 2013). fALFF values in the posterior lobe of the cerebellum and superior temporal gyrus change in patients with IGD, which may have

effects on executive functioning and movement flexibility (Lin, Jia, Zang, & Dong, 2015).

Multiple EEG studies have been published regarding IGD (Park et al., 2021). An event-related potential (ERP) study showed that the individuals with IGD had reduced P3 amplitude of the ERP at midline centro-parietal sites compared with HCs, which reflected cognitive deficiencies in patients with IGD (M. Park et al., 2016). The P3 component of ERPs derived from the EEG signal has been widely used to investigate brain functions and is regarded as an index of various cognitive processes (e.g., executive functioning, attention, and working memory) (Polich & Herbst, 2000). Some human lesion studies reported that the frontal, parietal, and temporal regions are associated with the P3 components (Bledowski et al., 2004; Knight, Scabini, Woods, & Clayworth, 1989; Kok, 2001). Many studies have revealed that P3 generators are involved in multiple neural circuits in the temporal, parietal, and precuneus brain regions (Mulert et al., 2004; Soltani & Knight, 2000; Volpe et al., 2007), although the exact neural origins of the P3 are not clearly known (O'Connell et al., 2012; Polich, 2007).

In healthy people at rest, the fMRI BOLD signal is associated with fluctuations of EEG power in various frequency bands (Mantini, Perrucci, Del Gratta, Romani, & Corbetta, 2007; Scheeringa et al., 2008). Simultaneous EEG-fMRI studies have shown that healthy people at rest have positive or negative associations between the fMRI BOLD signals and alpha power activity in the DMN region and the occipital cortex (Goldman, Stern, Engel, & Cohen, 2002; Jann et al., 2009).

Many studies have used either fMRI or EEG techniques to investigate IGD, but few multimodal studies have been conducted with a focus on regional activity in resting-state fMRI and ERPs. Thus, there is a need to examine whether the regional activity in resting-state fMRI is associated with ERP components; this information will help to characterize the neural relationships that underlie IGD. In this study, we used the ReHo, ALFF, and fALFF values of resting-state fMRI, as well as auditory oddball ERPs, to investigate neural and neurophysiological features of IGD, along with the neural correlates of those features. We hypothesized that patients with IGD would have abnormalities in resting-state fMRI and ERP features in brain regions associated with cognitive functioning and sensory processing; we presumed that these dysfunctional features would have neural correlates.

MATERIALS AND METHODS

Participants and clinical assessments

Twenty-six male individuals with IGD and 27 age- and intelligence quotient-matched male HCs were enrolled in this study. All individuals (aged 18 and 39 years) with IGD had presented to an outpatient clinic of SMG-SNU Boramae Medical Center, Seoul, South Korea, for the treatment of excessive and problematic internet gaming activities. The

participants were interviewed by an experienced psychiatrist for the diagnosis of IGD and comorbid psychiatric disorders based on criteria in the Diagnostic and Statistical Manual of Mental Disorders, Fifth Edition (DSM-5). IGD severity was assessed using Young's Internet Addiction Test (Young, 1996). All participants were medication-naive at the time of the assessment. None of the individuals with IGD had co-morbid psychiatric diagnoses. Individuals with IGD engaged in internet gaming for >4 h per day and >30 h per week; HCs engaged in internet gaming for <2 h per day. For all participants, the exclusion criteria were a history of head injury, neurological disease, psychiatric or psychotic disorder, and an estimated intelligence quotient score <80 according to the Korean version of the Wechsler Adult Intelligence Scale.

Resting-state fMRI acquisition

fMRI data were acquired using a Philips Achieva 3T MRI scanner (Philips Medical Systems, Best, Netherlands) with a standard whole-head coil. Functional data were obtained using a T2*-weighted echo-planar image sequence (slice thickness = 4 mm, in-plane dimension = 144×144, 35 slices, field of view = 220×220 mm, voxel size = $1.53 \times 1.53 \times 4$ mm, repetition time = 2,700 ms, echo time = 35 ms, and flip angle = 90°; 180 volumes). Participants were asked to rest with their eyes open, to remain awake, and to not think about anything specific during the fMRI scan. The anatomical images were acquired using a T1-weighted spoiled gradient-recalled three-dimensional MRI sequence (repetition time = 9.9 ms, echo time = 4.6 ms, slice thickness = 1.0 mm, flip angle = 8°, field of view = 220×220 mm, and voxel size = $1 \times 1 \times 1$ mm; 224 slices).

Resting-state fMRI preprocessing

Functional resting images were preprocessed using the Data Processing Assistant for Resting-State fMRI (http://www.restfmri.net, version 5.0) (Chao-Gan & Yu-Feng, 2010), implemented in MATLAB (MathWorks, Natick, MA, USA). The first 10 functional images were discarded for signal equilibration. The remaining 170 volumes were subjected to slice timing correction and realignment via six-parameter rigid-body spatial transformation. Data from individuals with an estimated head motion >2.0 mm of maximal rotation and 2.0° of any angular motion during the scan were excluded from further analysis. All data were spatially normalized to the Montreal Neurological Institute space and resampled in an isotropic voxel size of 3 mm. ReHo, ALFF, and fALFF values were calculated from resting-state fMRI data. Data from 3 IGD group and 2 HCs were excluded from the resting-state fMRI and EEG analysis in accordance with the above criteria.

Calculation of ReHo

The Friston 24 motion parameters, white matter, and cerebrospinal fluid were regressed as nuisance variables from the normalized BOLD signal before calculation of ReHo. To correct for excessive head motion, scrubbing procedures were used for volumes with a framewise displacement value >0.5. This involves scrubbing the time points one frame before and two frames after the bad point. We used the method of using each bad point as a separate regressor. Images were detrended to remove linear trends and temporally band-pass filtered (0.01–0.1 Hz) to reduce high-frequency physiological noise. ReHo maps were calculated with Kendall's coefficient of concordance. Each voxel was calculated with its 26-voxel neighborhood (Zang et al., 2004). For standardization, individual ReHo maps were divided by the global mean ReHo value within the whole brain mask.

Calculation of ALFF and fALFF

Spatial smoothing of normalized data was performed with a 4-mm full-width-half-maximum Gaussian kernel before calculation of ALFF and fALFF. The Friston 24 motion parameters, white matter, and cerebrospinal fluid were regressed out as nuisance variables from the smoothed images. Scrubbing procedures were performed. Finally, linear trends were removed during preprocessing for ALFF and fALFF, and then band-pass filtering (0.01–0.1 Hz) was performed during preprocessing. The time series for each voxel was transformed into the frequency domain using a fast Fourier transform method, and the mean square root of the power spectrum was obtained for the ALFF calculation. The fALFF value was calculated as the ratio of the amplitude within the low frequency (0.01–0.1 Hz) to the amplitude of the entire frequency range.

Auditory oddball task and EEG

EEG was conducted in a dimly lit, electrically shielded room. In accordance with the modified International 10–20 system, EEG signals were recorded using 64 Ag/AgCl electrodes (NeuroScan SynAmps2; Compumedics USA, El Paso, TX, USA) with a sampling rate of 1,000 Hz. Reference electrodes were linked to the mastoids, and the ground electrode was located between the FPz and Fz electrode sites. Horizontal electrooculogram signals were recorded with electrodes on the left and right eyes, whereas vertical electrooculogram electrodes were attached above and below the left eye. Impedances were set at < 5 kΩ. Participants were seated in a comfortable chair, then instructed to relax and avoid body movements throughout the experiment. The auditory oddball task required participants to press a response button for infrequently presented deviant stimuli (15%) and demonstrate a withdrawal response for standard stimuli (85%). The task consisted of three blocks of 100 trials each. In total, 300 stimuli comprised deviant stimuli (high-frequency tone of 2,000 Hz) and standard stimuli (low-frequency tone of 1,000 Hz) at 85 dB SPL, with 10 ms rise and fall times; the stimuli were presented binaurally through earphones in a pseudorandomized order, using a STIM 2 sound generator (Compumedics). The duration of each stimulus was 100 ms, and each intertrial interval was 1,250 ms. Response speed and accuracy were equally emphasized.

ERP analysis

Electrophysiological signals were preprocessed using Curry 7 software. The electrophysiological data were re-referenced to a common mean reference and band-pass filtered between 0.1 and 30 Hz. The data were visually inspected by an expert who detected and excluded gloss artifacts, such as movement. Eye blinks and eye movements were reduced based on a regression method implemented in Curry 7 (Semlitsch, Anderer, Schuster, & Presslich, 1986). Continuous EEG data were epoched from 100 ms before the stimulus to 900 ms after the stimulus. Baseline correction was conducted using the mean amplitude before stimulus onset. Single-trial epochs from any channel with voltages $> \pm 70 \mu V$ were automatically excluded from further analysis. Only artifact-free epochs and correct responses to infrequent stimuli at midline centro-parietal sites (CPz and Pz) were averaged and analyzed. The P3 component was defined as the largest positive deflection in the time range from 248 to 500 ms after stimulus onset.

Statistical analysis

Demographic and clinical characteristics, as well as behavioral data, were compared between groups using an independent two-sample t-test.

Statistical analyses for the resting-stage fMRI ReHo, ALFF, and fALFF maps were performed in SPM12 (http://www.fil.ion.ucl.ac.uk/spm). To evaluate between-group differences on the ReHo, ALFF, and fALFF maps, two-sample t-tests were performed in a voxel-by-voxel manner. Age was included as a nuisance variable to remove the residual effect. Regression analysis was conducted after controlling for age to determine associations of the ReHo, ALFF, and fALFF maps with P3 amplitudes from the oddball task. We had further performed regression analyzes to determine the association of ReHo, ALFF, and fALFF values with Beck Depression Inventory (BDI) or Beck Anxiety Inventory (BAI) scores in IGD individuals. In fMRI analysis, clinical features such as BDI or BAI are not considered nuisance variables in our study. Since clinical features such as BDI and BAI can be characteristics in the individuals with IGD, examining the brain functions related to the clinical features rather than controlling the characteristics themselves can determine the difference between the individuals with IGD

and the normal group. An uncorrected p-value <0.001 with a minimum cluster size of 10 contiguous voxels was considered statistically significant.

We performed correlation analysis to determine the associations of IGD symptom severity with the region of interest in the ReHo, ALFF, and fALFF maps showing significant group differences of fMRI, using Pearson's correlation analysis with SPSS software, ver. 25.0 (SPSS Inc., Chicago, IL, USA).

In the auditory oddball ERP task, repeated-measures analysis of variance was performed for the amplitudes and latencies of the P3 component, with the electrode site as the within-subject factor and group as the between-subject factor. Additionally, Pearson's correlation analysis was conducted to identify relationships between P3 components with group differences and IGD severity scores in individuals with IGD. All statistical analyses were two-tailed, and P-values <0.05 were considered statistically significant.

Ethics

The institutional review board of SMG- SNU Boramae Medical Center approved the study protocol, and the study followed the guidelines of the Declaration of Helsinki. All participants understood the study procedure and provided written informed consent.

RESULTS

Demographic data

The demographic and clinical characteristics of the participants are presented in Table 1. The two groups did not differ in terms of age or intelligence quotient. However, they significantly differed in terms of the duration of education, as well as the Young's Internet Addiction Test, BDI, and BAI scores.

ERP and behavioral results

Analysis of P3 amplitudes revealed a significant main effect of group [F (1, 43) = 5.242, p = 0.027, η_p^2 = 0.109]. No main effect of electrode site was observed, and no interaction with P3 amplitudes was detected. Compared with HCs,

Table 1. Demographic characteristics, clinical characteristics, and behavioral data of study participants

	Healthy control (n = 25) Mean (SD)	Internet gaming disorder (n = 23) Mean (SD)	t	p
Age (year)	25.04 (3.86)	23.13 (5.21)	1.45	0.15
IQ	118.28 (9.56)	118.52 (11.87)	−0.08	0.94
Young's Internet Addiction Test (IAT)	27.83 (8.29)	72.22 (12.76)	−14.20	<0.001***
BDI	3.17 (3.29)	19.74 (9.96)	−7.59	<0.001***
BAI	4.83 (5.27)	16.78 (14.16)	−3.80	0.001**
Accuracy (%)	98.49 (2.70)	97.98 (4.11)	0.51	0.98
Reaction Time (ms)	351.80 (43.43)	351.53 (39.16)	0.02	0.98

Abbreviations: ** indicates $p < 0.01$; *** indicates $p < 0.001$; SD, standard deviation; IQ, intelligence quotient; BDI, Beck Depression Inventory; BAI, Beck Anxiety Inventory.

individuals with IGD had significantly lower P3 amplitudes at CPz [$F(1, 43) = 5.823$, $p = 0.020$, $\eta_p^2 = 0.119$], but not at Pz (Fig. 1). No main effect of electrode site and no interaction with P3 latency was observed. The average number of trials for the P3 component is 35.74 trials, and no group difference was found in the number of trials for the P3 component ($t = 0.656$, $p = 0.515$, HC; mean = 36.14, sd = 4.04 vs. IGD: mean = 35.33 sd = 3.98). No differences in accuracy or reaction times on the auditory oddball task were observed between the two groups.

Group differences in regional activity of fMRI (ReHo, ALFF, and fALFF) maps

Group differences in the ReHo, ALFF, and fALFF values are shown in Fig. 1 and Table 2. Compared with HCs, a significant
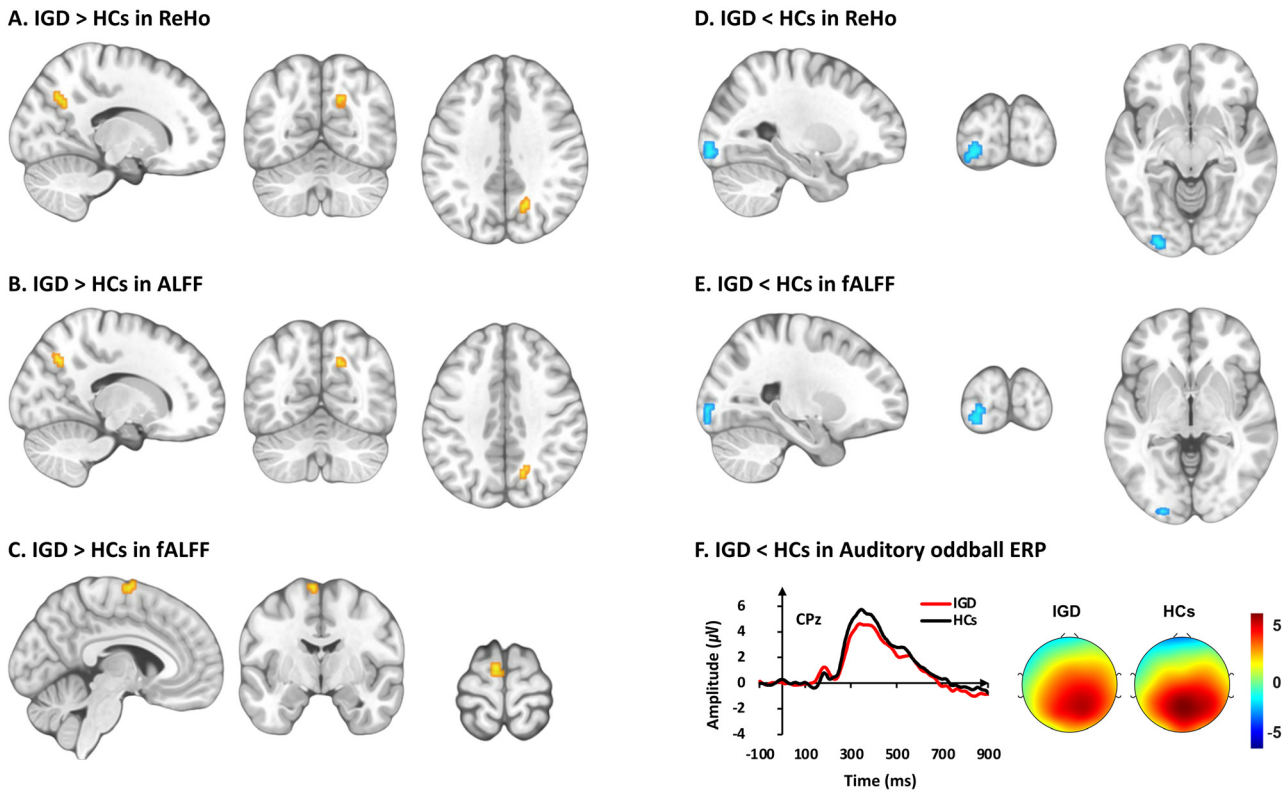

Fig. 1. Group differences in regional activity of resting-state fMRI (ReHo, ALFF, and fALFF) and P3 amplitudes of auditory oddball ERP between patients with Internet gaming disorder (IGD) and healthy controls (HCs). Brain regions with significant changes in regional fMRI between patients with IGD and HCs. IGD patients showed increased resting-state fMRI activities in warm-colored brain regions and decreased activities in cool-colored brain regions. Compared with HCs, the IGD group had significantly increased ReHo (A) and ALFF (B) values in the right precuneus, and increased fALFF (C) in the left superior frontal gyrus. The IGD group exhibited significant increases of ReHo (D) and fALFF (E) values in the left inferior occipital gyrus. (F) Grand-average ERP waveforms at the midline centro-parietal area and topographic maps indicating scalp distribution of P3 amplitudes in two groups
*Abbreviations: ReHo, regional homogeneity; ALFF, amplitude of low-frequency fluctuation; fALFF, fractional amplitude of low-frequency fluctuation; ERPs, event related potentials; CPz, midline centro-parietal.

Table 2. Brain regions with significant differences in regional fMRI (ReHo, ALFF, and fALFF) between patients with internet gaming disorder (IGD) and healthy controls (HC)

Condition	Region	Peak MNI coordinates			T-values	voxels
		x	y	z		
IGD > HC in ReHo	R. precuneus	15	−63	36	4.09	15
IGD > HC in ALFF	R. precuneus	15	−63	39	4.02	10
IGD > HC in ALFF	L. superior frontal gyrus	−6	−6	72	4.07	12
HC > IGD in ReHo	L. inferior occipital gyrus	−27	−93	−9	4.12	21
HC > IGD in fALFF	L. inferior occipital gyrus	−24	−96	−3	4.41	11

Abbreviations: ReHo, regional homogeneity; ALFF, amplitude of low-frequency fluctuation; fALFF, fractional amplitude of low-frequency fluctuation; MNI, Montreal Neurological Institute ($p < 0.001$, uncorrected, cluster threshold ≥10).
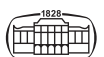
decrease in ReHo was detected in the left inferior occipital gyrus (IOG)/occipital fusiform gyrus in individuals with IGD, whereas an increase in the right precuneus was observed. Individuals with IGD exhibited significant increases in ALFF in the left superior frontal gyrus (SFG) and right precuneus, compared with HCs. Additionally, individuals with IGD had significantly lower fALFF in the left IOG, compared with HCs.

Correlations between P3 amplitudes and regional activity of fMRI (ReHo, ALFF, and fALFF) maps

The relationships of P3 amplitudes with regional activity in the ReHo, ALFF, and fALFF maps are shown in Fig. 2 and Table 3. In the IGD group, significant positive correlations were found between ReHo and P3 amplitudes at CPz in the right inferior temporal gyrus (ITG), right medial orbital gyrus, right lingual gyrus, right calcarine cortex, and right superior occipital gyrus; negative correlations were found in the left hippocampus and right amygdala. A significant positive correlation was observed between ALFF and P3 amplitudes in the right calcarine cortex/lingual gyrus in the IGD group, whereas a positive correlation was detected in the left postcentral gyrus/precentral gyrus in HCs. Additionally, a positive correlation was observed between fALFF and P3 amplitudes in the right lingual gyrus/calcarine cortex in the IGD group.

Correlations between IGD symptom severity and ROI values of regional activity of fMRI (ReHo, ALFF, and fALFF) or P3 amplitudes in individuals with IGD

We found no significant correlations between IGD symptom severity and regional activity of fMRI (ReHo, ALFF, and fALFF) or P3 amplitudes in individuals with IGD. ROI values in the precuneus of ReHo ($r = 0.140$, $p = 0.524$) and ALFF ($r = 0.087$, $p = 0.693$) were not associated with IGD symptom severity in individuals with IGD. ROI values in the left SFG of ALFF ($r = -0.087$, $p = 0.694$) or left IOG of ReHo ($r = -0.349$, $p = 0.103$) and fALFF ($r = -0.080$, $p = 0.716$) were not associated with IGD symptom severity in individuals with IGD.

Correlations between BDI or Bai scores and regional activity of fMRI (ReHo, ALFF, and fALFF) maps

We found that BDI scores were negatively associated with ReHo and fALFF values of the occipital area, and BAI scores were also negatively associated with fALFF of the occipital area (shown in Table 4).

DISCUSSION

This study was performed to investigate neural features and neural correlates between regional activity of resting-state fMRI (ReHo, ALFF, and fALFF) and auditory oddball ERPs in individuals with IGD. To our knowledge, this is the first study to utilize multimodal technologies that combined regional neural activity in resting-state fMRI and ERPs to provide insights into the neural correlates that underlie IGD. We demonstrated that individuals with IGD had altered regional activity of resting-state fMRI and reduced P3 amplitudes of ERPs. Additionally, we detected a correlation between the spontaneous regional activity and P3 amplitudes of ERPs at CPz in the IGD group.

Analyses of regional activity in resting-state fMRI revealed that individuals with IGD had higher ReHo and ALFF values in the right precuneus and increased ALFF in the left SFG, compared with HCs. In contrast, the individuals with exhibited lower ReHo and fALFF values in the left IOG, compared with HCs. ALFF and fALFF both analyze low-frequency fluctuations in the BOLD signal, but ALFF is sensitive to local neural activity, while fALFF, a normalized version of ALFF, is considered to provide a physiologically-adjusted measure of regional brain activity, reducing potential confounds caused by global signal fluctuations. Although some group differences were found in ALFF and fALFF values, the brain regions where group differences were found in ReHo values were also found in the same area ALFF and fALFF values, respectively. These results are consistent with the findings in previous studies (Dong et al., 2012; Kim et al., 2015). The precuneus plays a key role in the DMN and is associated with various cognitive functions (Cavanna & Trimble, 2006; Fransson & Marrelec, 2008; Utevsky, Smith, & Huettel, 2014). An ERP study demonstrated activation of the precuneus in deviant P3 compared with standard P3, suggesting an increase in attentional demands from top-down control (Justen & Herbert, 2018). Adolescents with IGD have higher ALFF values in the precuneus and orbitofrontal cortex (OFC) (Yuan, Jin, et al., 2013), and a positive correlation has been observed between ReHo in the precuneus and IGD symptom severity in patients with IGD (H. Kim et al., 2015). A structural study showed that adolescents with IGD develop increased cortical thickness in the precuneus and temporal cortex, as well as decreased cortical thickness in the OFC and lingual gyrus (Yuan, Cheng, et al., 2013). A recent study of patients with IGD suggested that the precuneus serves as a hub for integrating information between executive control and subcortical cravings (Dong et al., 2020).

The SFG is involved in top-down cognitive control of behavior, including decision-making, selective attention, inhibitory control, cravings, and motor control (Corbetta & Shulman, 2002; Hopfinger, Buonocore, & Mangun, 2000). Patients with IGD have aberrant functional activity and connectivity in the SFG (Wang et al., 2015). Adolescents with IGD reportedly exhibit greater response inhibition activity in the SFG, while SFG activation is correlated with symptom severity and impulsivity scores; thus, adolescents with IGD may exhibit decreased response inhibition and prefrontal cortex dysfunction (Ding et al., 2014).

The lower ReHo and fALFF values in the left IOG suggest that individuals with IGD have decreased synchronization and intensity of regional activity in occipital areas, compared with HCs. The occipital lobe is a key visual processing area. There are also reports that the visual cortex is activated by auditory attention (Cate et al., 2009; McDonald,
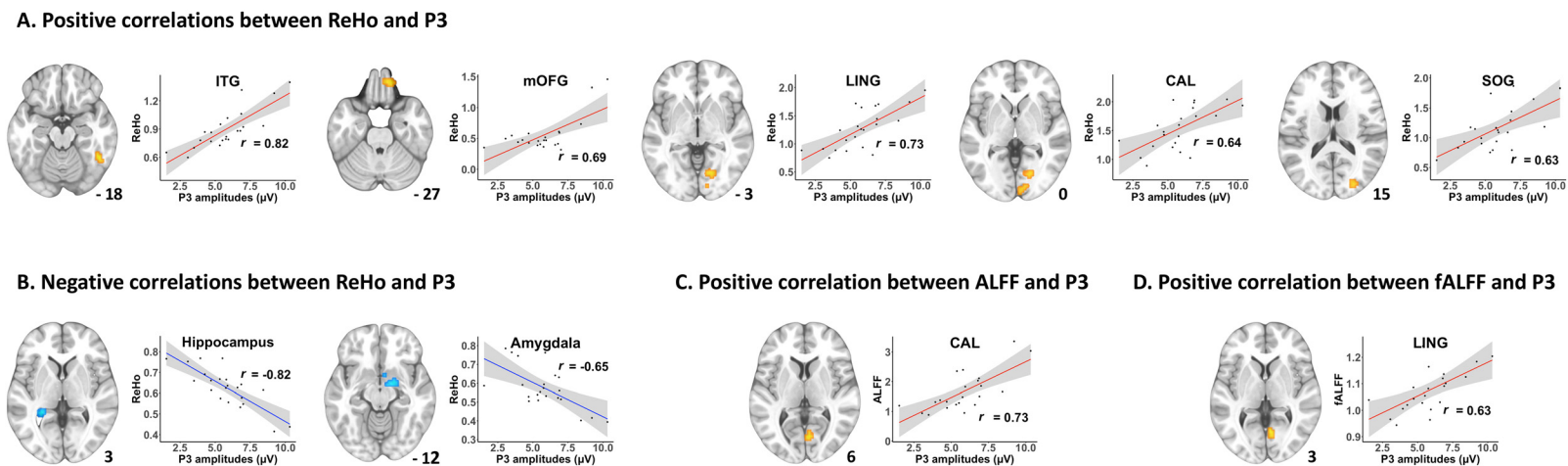
Fig. 2. Brain regions showing correlations between regional activity of resting-state fMRI (ReHo, ALFF, and fALFF) and P3 amplitudes of auditory oddball ERP in patients with Internet gaming disorder (IGD) and those scatter plots. ReHo, ALFF, and fALFF maps of resting-state fMRI were correlated with P3 amplitudes of ERPs in the IGD group. A Warm-colored brain regions and scatter plots display mean positive correlations between ReHo and P3 amplitudes at the midline centro-parietal (CPz) area of auditory oddball ERP in IGD. B Cool-colored brain regions and scatter plots display mean negative correlations between ReHo and P3 amplitudes at CPz in IGD. C Warm-colored brain regions and scatter plots display mean positive correlations between ALFF and P3 amplitudes at CPz in IGD. D Warm-colored brain regions and scatter plots display mean positive correlations between fALFF and P3 amplitudes at CPz in IGD

Abbreviations: ReHo, regional homogeneity; ALFF, amplitude of low-frequency fluctuation; fALFF, fractional amplitude of low-frequency fluctuation; ERPs, event related potentials; ITG, inferior temporal gyrus; mOFC, medial orbitofrontal cortex; LING, lingual gyrus; CAL, calcarine cortex; SOG, superior occipital gyrus.

Table 3. Associations of resting-state fMRI (ReHo, ALFF, and fALFF) with P3 amplitudes

Condition	Region	Peak MNI coordinates			T-values	voxels
		x	y	z		
Positive correlation in IGD						
ReHo	R. inferior temporal gyrus	48	−51	−18	6.30	19
ReHo	R. medial orbital gyrus	12	45	−27	5.10	24
ReHo	R. lingual gyrus	18	−72	−3	4.94	22
ReHo	R. calcarine cortex	6	−93	0	4.27	11
ReHo	R. superior occipital gyrus	27	−84	15	4.26	10
ALFF	R. calcarine cortex	6	−72	6	5.91	25
fALFF	R. lingual gyrus	6	−63	3	4.88	27
Negative correlation in IGD						
ReHo	L. Hippocampus	−27	−42	3	6.30	14
ReHo	R. Amygdala	18	−3	−12	5.24	35

Abbreviations: ReHo, regional homogeneity; ALFF, amplitude of low-frequency fluctuation; fALFF, fractional amplitude of low-frequency fluctuation; MNI, Montreal Neurological Institute; IGD, internet gaming disorder; R, right; L, left ($p < 0.001$, uncorrected, cluster threshold ≥10).

Table 4. Correlations between regional activity of fMRI and depression or anxiety scores in individuals with IGD

Condition	Region	Peak MNI coordinates			T-values	voxels
		x	y	z		
Negative correlation between fMRI and BDI						
ReHo	L. calcarine cortex	−15	−78	15	4.74	113
ReHo	R. inferior occipital gyrus	51	−75	−6	4.37	13
ALFF	L. cuneus	−3	−84	24	5.75	35
fALFF	L. superior occipital gyrus	−18	−81	15	5.75	31
fALFF	L. calcarine cortex	0	−102	0	4.80	16
fALFF	R. calcarine cortex	15	−66	9	4.79	12
Negative correlation between fMRI and BAI						
ReHo	R. middle cingulate gyrus	6	−16	45	4.99	10
fALFF	R. inferior occipital gyrus	27	−93	3	5.26	10
fALFF	R. lingual gyrus	18	−93	3	5.02	13

Abbreviations: ReHo, regional homogeneity; ALFF, amplitude of low-frequency fluctuation; fALFF, fractional amplitude of low-frequency fluctuation; MNI, Montreal Neurological Institute; IGD, internet gaming disorder; R, right; L, left ($p < 0.001$, uncorrected, cluster threshold ≥10).

Stormer, Martinez, Feng, & Hillyard, 2013). Individuals with IGD had lower regional activity in the occipital region; this finding may have been affected by excessive exposure to auditory and visual stimuli over a long period. These findings are consistent with the results of a previous ReHo study, in which IGD patients exhibited lower ReHo values in temporal, occipital, and parietal regions (Dong et al., 2012).

The higher ReHo and ALFF values in the right precuneus and left SFG, and the lower ReHo and fALFF values in the left IOG, represent changes in regional synchronization and intensity in these regions in individuals with IGD; such changes suggest impairments in the DMN and cognitive function, as well as dysfunctional sensory processing. These results also suggest that individuals with IGD are likely to have an imbalance between top-down cognitive control and bottom-up sensory processing.

Compared with HCs, individuals with IGD had lower P3 amplitudes at CPz area on the auditory oddball task, which is regarded as an index of cognitive resources (Park et al., 2016);

this finding indicated that patients with IGD had cognitive and sensory dysfunction.

The present study focused on the relationship between regional neural activity on resting-state fMRI and ERPs during a cognitive task in individuals with IGD. The regional activity of resting-state fMRI in the right ITG, OFC, and occipital cortex (e.g., right lingual gyrus, calcarine cortex, and superior occipital gyrus) was positively correlated with the P3 amplitudes of ERPs in individuals with IGD. Additionally, ReHo activities in the left hippocampus and right amygdala were negatively correlated with P3 amplitudes in the IGD group. These relationships between the low-frequency resting-state BOLD signal and activity-related ERP confirmed that fMRI brain activity under task-independent conditions was associated with activity levels in task-relevant ERPs, even when different neuroimaging modalities were used. These findings may be related to the lack of active interaction between brain regions.

The ITG is presumed to play a central role in cognitive processing, including semantic memory, language, certain

aspects of visual perception, and multimodal and higher sensory processing (Mesulam, 1998; Onitsuka et al., 2004). Previous neuroimaging studies have identified changes in the superior and ITG, as well as the occipital cortex, in patients with IGD (Yuan, Cheng, et al., 2013). The OFC, with connections to the prefrontal, limbic, and sensory areas, is involved in various human behaviors (Bechara, Damasio, & Damasio, 2000; Schoenbaum, Roesch, & Stalnaker, 2006). OFC dysfunction and connectivity play a role in the deviant behaviors associated with addictive disorders (Kim et al., 2019; London, Ernst, Grant, Bonson, & Weinstein, 2000; Volkow & Fowler, 2000). An ^{18}F-fluorodeoxyglucose positron emission tomography study revealed increased glucose metabolism in the OFC and striatum of the IGD group; these changes were related to the dopaminergic system (Park et al., 2010). Individuals with IGD had decreased gray matter volume in the OFC (Jin et al., 2016; Weng et al., 2013) and decreased cortical thickness in the OFC (Hong et al., 2013), suggesting changes in the neural mechanism that underlies cognitive behavioral performance. The positive correlation between the P3 amplitudes and regional activity of resting-state fMRI in the prefrontal, temporal, and occipital cortices suggests that cognitive processing of tasks is inefficient in individuals with IGD when their auditory and visual processing integration capacity decreases during the resting state. Also, we found that higher depression or anxiety scores in individuals with IGD correlated with lower ReHo and fALFF values of regional resting-state fMRI activity in the occipital area. We found lower ReHo and fALFF values of the occipital regions in individuals with IGD correlated with lower the P3 amplitudes. Additionally, we found that individuals with IGD showed lower ReHo and fALFF values in the occipital area. These findings suggest that the lower ReHo and fALFF values of the fMRI activity in the occipital regions, which are also associated with cognitive functions as well as sensory systems in individuals with IGD, are associated with the characteristics of individuals with IGD.

Furthermore, the P3 amplitudes of ERPs in individuals with IGD were negatively correlated with the regional ReHo activity in the left hippocampus and right amygdala. Interactions between the hippocampus and amygdala are important in emotional memory and learning (Robbins, Ersche, & Everitt, 2008; Volkow et al., 2010). Neuroimaging studies have revealed that the hippocampus and amygdala are associated with cravings in response to addiction-related cues (Childress et al., 1999; Grant et al., 1996; Sun et al., 2012). There is evidence that exposure to drug-related cues is associated with the activation of dopamine transmission in the amygdala and hippocampus (Fotros et al., 2013; Weiss et al., 2000). Patients with IGD had larger volumes in the precuneus and hippocampus/amygdala; hippocampal volume is reportedly correlated with symptom severity in IGD and may be influenced by internet gaming-related cues (Yoon et al., 2017). Compared with HCs, IGD patients reportedly exhibited higher resting-state functional connectivity between the amygdala and dorsolateral prefrontal cortex, which was negatively associated with depression symptom severity within the IGD group (Liu et al., 2018). A task fMRI study showed that IGD patients with major depressive disorder had greater relative activation in the hippocampus during an attention task, compared with the pure IGD group and HCs; this finding suggested that IGD patients with major depressive disorder could not suppress brain activity within the DMN (Han, Kim, Bae, Renshaw, & Anderson, 2016).

The findings of negative correlations between P3 amplitudes and ReHo activation in the hippocampus and amygdala suggest that dysfunctional cognitive processing in individuals with IGD is associated with regional activity in the hippocampus and amygdala that are involved in conditioned learning and memory. Cognitive impairment in individuals with IGD is associated with the weakening of hippocampus and amygdala functionality in response to the cumulative experience of internet gaming habits and emotional memory. The hippocampus and amygdala are involved with emotional processing and may modulate or interact with other brain regions; therefore, careful interpretation and further investigations are needed.

Some limitations of this study should be noted. First, because the current study was cross-sectional, it is difficult to establish causality or directionality. A longitudinal study may help to clarify causality. Second, because the participants were all younger men, our findings may be not generalizable to other populations. Third, because the current study has not found that individuals with IGD have any cognitive or sensory difficulties at the level of behavior, this study should be interpreted with some caution. Fourth, because BDI or BAI scores were uncontrollable, the effects of depression and anxiety are difficult to exclude completely, but none of the individuals with IGD who participated in this study had psychiatric comorbidities. However, the current study had a few notable strengths. This is the first multimodal study to combine resting-state fMRI with ERPs during a cognitive task in individuals with IGD.

In summary, this multimodal study of combined regional activity during resting-state fMRI and auditory oddball task ERPs revealed that resting-state regional brain hemodynamics are associated with ERP neuronal activities, particularly in brain areas involved in cognition, sensory, and emotional modulation and integration. These findings suggest that individuals with IGD patients have an imbalance between top-down and bottom-up processing, which hinders efficient cognitive and sensory processing in these patients. Therefore, we suggest that characteristics of IGD with high levels of game-related conditions and loss of control make it difficult for IGD patients to maintain a proper gaming life balance, which may lead to continuous game behavior. We expect that these findings will broaden the understanding of neural mechanisms that underlie IGD pathophysiology and will facilitate clinical interventions to improve the mental well-being of individuals who may develop IGD.

REFERENCES

Bechara, A., Damasio, H., & Damasio, A.R. (2000). Emotion, decision making and the orbitofrontal cortex. *Cereb Cortex*, *10*(3), 295–307. https://doi.org/10.1093/cercor/10.3.295.

Bledowski, C., Prvulovic, D., Hoechstetter, K., Scherg, M., Wibral, M., Goebel, R., & Linden, D. E. (2004). Localizing P300 generators in visual target and distractor processing: A combined event-related potential and functional magnetic resonance imaging study. *Journal of Neuroscience*, *24*(42), 9353–9360. https://doi.org/10.1523/JNEUROSCI.1897-04.2004.

Cate, A. D., Herron, T. J., Yund, E. W., Stecker, G. C., Rinne, T., Kang, X., … Woods, D. L. (2009). Auditory attention activates peripheral visual cortex. *Plos One*, *4*(2), e4645. https://doi.org/10.1371/journal.pone.0004645.

Cavanna, A. E., & Trimble, M. R. (2006). The precuneus: A review of its functional anatomy and behavioural correlates. *Brain*, *129*(Pt 3), 564–583. https://doi.org/10.1093/brain/awl004.

Chao-Gan, Y., & Yu-Feng, Z. (2010). DPARSF: A MATLAB toolbox for "Pipeline" data analysis of resting-state fMRI. *Frontiers in Systems Neuroscience*, *4*, 13. https://doi.org/10.3389/fnsys.2010.00013.

Childress, A. R., Mozley, P. D., McElgin, W., Fitzgerald, J., Reivich, M., & O'Brien, C. P. (1999). Limbic activation during cue-induced cocaine craving. *American Journal of Psychiatry*, *156*(1), 11–18. https://doi.org/10.1176/ajp.156.1.11.

Corbetta, M., & Shulman, G. L. (2002). Control of goal-directed and stimulus-driven attention in the brain. *Nature Reviews. Neuroscience*, *3*(3), 201–215. https://doi.org/10.1038/nrn755.

Ding, W. N., Sun, J. H., Sun, Y. W., Chen, X., Zhou, Y., Zhuang, Z. G., … Du, Y. S. (2014). Trait impulsivity and impaired prefrontal impulse inhibition function in adolescents with internet gaming addiction revealed by a Go/No-Go fMRI study. *Behavioral and Brain Functions*, *10*(1), 20. https://doi.org/10.1186/1744-9081-10-20.

Dong, G., Huang, J., & Du, X. (2012). Alterations in regional homogeneity of resting-state brain activity in internet gaming addicts. *Behavioral and Brain Functions*, *8*(1), 41. https://doi.org/10.1186/1744-9081-8-41.

Dong, G. H., Wang, M., Wang, Z., Zheng, H., Du, X., & Potenza, M. N. (2020). Addiction severity modulates the precuneus involvement in internet gaming disorder: Functionality, morphology and effective connectivity. *Progress in Neuro-Psychopharmacology & Biological Psychiatry*, *98*, 109829. https://doi.org/10.1016/j.pnpbp.2019.109829.

Fotros, A., Casey, K. F., Larcher, K., Verhaeghe, J. A., Cox, S. M., Gravel, P., … Leyton, M. (2013). Cocaine cue-induced dopamine release in amygdala and hippocampus: A high-resolution PET [^{18}F]fallypride study in cocaine dependent participants. *Neuropsychopharmacology*, *38*(9), 1780–1788. https://doi.org/10.1038/npp.2013.77.

Fransson, P., & Marrelec, G. (2008). The precuneus/posterior cingulate cortex plays a pivotal role in the default mode network: Evidence from a partial correlation network analysis. *Neuroimage*, *42*(3), 1178–1184. https://doi.org/10.1016/j.neuroimage.2008.05.059.

Goldman, R. I., Stern, J. M., Engel, J., Jr., & Cohen, M. S. (2002). Simultaneous EEG and fMRI of the alpha rhythm. *Neuroreport*, *13*(18), 2487–2492. https://doi.org/10.1097/01.wnr.0000047685.08940.d0.

Grant, S., London, E. D., Newlin, D. B., Villemagne, V. L., Liu, X., Contoreggi, C., … Margolin, A. (1996). Activation of memory circuits during cue-elicited cocaine craving. *Proceedings of the National Academy of Sciences of the United States of America*, *93*(21), 12040–12045. https://doi.org/10.1073/pnas.93.21.12040.

Han, D. H., Kim, S. M., Bae, S., Renshaw, P. F., & Anderson, J. S. (2016). A failure of suppression within the default mode network in depressed adolescents with compulsive internet game play. *Journal of Affective Disorders*, *194*, 57–64. https://doi.org/10.1016/j.jad.2016.01.013.

Han, Y., Wang, J., Zhao, Z., Min, B., Lu, J., Li, K., … Jia, J. (2011). Frequency-dependent changes in the amplitude of low-frequency fluctuations in amnestic mild cognitive impairment: A resting-state fMRI study. *Neuroimage*, *55*(1), 287–295. https://doi.org/10.1016/j.neuroimage.2010.11.059.

Hong, S. B., Kim, J. W., Choi, E. J., Kim, H. H., Suh, J. E., Kim, C. D., … Yi, S. H. (2013). Reduced orbitofrontal cortical thickness in male adolescents with internet addiction. *Behavioral and Brain FunctionsF*, *9*(1), 11. https://doi.org/10.1186/1744-9081-9-11.

Hopfinger, J. B., Buonocore, M. H., & Mangun, G. R. (2000). The neural mechanisms of top-down attentional control. *Nature Neuroscience*, *3*(3), 284–291. https://doi.org/10.1038/72999.

Hoptman, M. J., Zuo, X. N., Butler, P. D., Javitt, D. C., D'Angelo, D., Mauro, C. J., & Milham, M. P. (2010). Amplitude of low-frequency oscillations in schizophrenia: A resting state fMRI study. *Schizophrenia Research*, *117*(1), 13–20. https://doi.org/10.1016/j.schres.2009.09.030.

Jann, K., Dierks, T., Boesch, C., Kottlow, M., Strik, W., & Koenig, T. (2009). BOLD correlates of EEG alpha phase-locking and the fMRI default mode network. *Neuroimage*, *45*(3), 903–916. https://doi.org/10.1016/j.neuroimage.2009.01.001.

Jin, C., Zhang, T., Cai, C., Bi, Y., Li, Y., Yu, D., … Yuan, K. (2016). Abnormal prefrontal cortex resting state functional connectivity and severity of internet gaming disorder. *Brain Imaging and*

Behavior, *10*(3), 719–729. https://doi.org/10.1007/s11682-015-9439-8.

Justen, C., & Herbert, C. (2018). The spatio-temporal dynamics of deviance and target detection in the passive and active auditory oddball paradigm: A sLORETA study. *BMC Neuroscience*, *19*(1), 25. https://doi.org/10.1186/s12868-018-0422-3.

Kim, J. Y., Chun, J. W., Park, C. H., Cho, H., Choi, J., Yang, S., … Kim, D. J. (2019). The correlation between the frontostriatal network and impulsivity in internet gaming disorder. *Scientific Reports*, *9*(1), 1191. https://doi.org/10.1038/s41598-018-37702-4.

Kim, H., Kim, Y. K., Gwak, A. R., Lim, J. A., Lee, J. Y., Jung, H. Y., … Choi, J. S. (2015). Resting-state regional homogeneity as a biological marker for patients with internet gaming disorder: A comparison with patients with alcohol use disorder and healthy controls. *Progress in Neuro-Psychopharmacology & Biological Psychiatry*, *60*, 104–111. https://doi.org/10.1016/j.pnpbp.2015.02.004.

Knight, R. T., Scabini, D., Woods, D. L., & Clayworth, C. C. (1989). Contributions of temporal-parietal junction to the human auditory P3. *Brain Research*, *502*(1), 109–116. https://doi.org/10.1016/0006-8993(89)90466-6.

Kok, A. (2001). On the utility of P3 amplitude as a measure of processing capacity. *Psychophysiology*, *38*(3), 557–577. https://doi.org/10.1017/S0048577201990559.

Lin, X., Jia, X., Zang, Y. F., & Dong, G. (2015). Frequency-dependent changes in the amplitude of low-frequency fluctuations in internet gaming disorder. *Frontiers in Psychology*, *6*, 1471. https://doi.org/10.3389/fpsyg.2015.01471.

Liu, L., Yao, Y. W., Li, C. R., Zhang, J. T., Xia, C. C., Lan, J., … Fang, X. Y. (2018). The comorbidity between internet gaming disorder and depression: Interrelationship and neural mechanisms. *Frontiers in Psychiatry*, *9*, 154. https://doi.org/10.3389/fpsyt.2018.00154.

London, E. D., Ernst, M., Grant, S., Bonson, K., & Weinstein, A. (2000). Orbitofrontal cortex and human drug abuse: Functional imaging. *Cereb Cortex*, *10*(3), 334–342. https://doi.org/10.1093/cercor/10.3.334.

Mantini, D., Perrucci, M. G., Del Gratta, C., Romani, G. L., & Corbetta, M. (2007). Electrophysiological signatures of resting state networks in the human brain. *Proceedings of the National Academy of Sciences of the United States of America*, *104*(32), 13170–13175. https://doi.org/10.1073/pnas.0700668104.

McDonald, J. J., Stormer, V. S., Martinez, A., Feng, W., & Hillyard, S. A. (2013). Salient sounds activate human visual cortex automatically. *The Journal of Neuroscience*, *33*(21), 9194–9201. https://doi.org/10.1523/JNEUROSCI.5902-12.2013.

Mestre-Bach, G., Granero, R., Fernández-Aranda, F., Jiménez-Murcia, S., & Potenza, M. N. (2023). Independent component analysis for internet gaming disorder. *Dialogues in Clinical Neuroscience*, *25*(1), 14–23. https://doi.org/10.1080/19585969.2023.2168135.

Mesulam, M. M. (1998). From sensation to cognition. *Brain*, *121*(6), 1013–1052. https://doi.org/10.1093/brain/121.6.1013.

Mulert, C., Jager, L., Schmitt, R., Bussfeld, P., Pogarell, O., Moller, H. J., … Hegerl, U. (2004). Integration of fMRI and simultaneous EEG: Towards a comprehensive understanding of localization and time-course of brain activity in target

detection. *Neuroimage*, *22*(1), 83–94. https://doi.org/10.1016/j.neuroimage.2003.10.051.

Nunez, P. L., Srinivasan, R., Westdorp, A. F., Wijesinghe, R. S., Tucker, D. M., Silberstein, R. B., & Cadusch, P. J. (1997). EEG coherency. I: Statistics, reference electrode, volume conduction, Laplacian, cortical imaging, and interpretation at multiple scales. *Electroencephalography and Clinical Neurophysiology*, *103*(5), 499–515. https://doi.org/10.1016/s0013-4694(97)00066-7.

O'Connell, R. G., Balsters, J. H., Kilcullen, S. M., Campbell, W., Bokde, A. W., Lai, R. … Robertson, I. H. (2012). A simultaneous ERP/fMRI investigation of the P300 aging effect. *Neurobiology of Aging*, *33*(10), 2448–2461. https://doi.org/10.1016/j.neurobiolaging.2011.12.021.

Onitsuka, T., Shenton, M. E., Salisbury, D. F., Dickey, C. C., Kasai, K., Toner, S. K., … McCarley, R. W. (2004). Middle and inferior temporal gyrus gray matter volume abnormalities in chronic schizophrenia: An MRI study. *Am Journal of Psychiatry*, *161*(9), 1603–1611. https://doi.org/10.1176/appi.ajp.161.9.1603.

Park, M., Choi, J. S., Park, S. M., Lee, J. Y., Jung, H. Y., Sohn, B. K., … Kwon, J. S. (2016). Dysfunctional information processing during an auditory event-related potential task in individuals with Internet gaming disorder. *Translational Psychiatry*, *6*(1), e721. https://doi.org/10.1038/tp.2015.215.

Park, H. S., Kim, S. H., Bang, S. A., Yoon, E. J., Cho, S. S., & Kim, S. E. (2010). Altered regional cerebral glucose metabolism in internet game overusers: A 18F-fluorodeoxyglucose positron emission tomography study. *CNS Spectrums*, *15*(3), 159–166. https://doi.org/10.1017/s1092852900027437.

Park, M., Yoo, S. Y., Lee, J. Y., Koo, J. W., Kang, U. G., & Choi, J. S. (2021). Relationship between resting-state alpha coherence and cognitive control in individuals with internet gaming disorder: A multimodal approach based on resting-state electroencephalography and event-related potentials. *Brain Science*, *11*(12), 1635. https://doi.org/10.3390/brainsci11121635.

Polich, J. (2007). Updating P300: An integrative theory of P3a and P3b. *Clinical Neurophysiology*, *118*(10), 2128–2148. https://doi.org/10.1016/j.clinph.2007.04.019.

Polich, J., & Herbst, K. L. (2000). P300 as a clinical assay: Rationale, evaluation, and findings. *International Journal of Psychophysiology*, *38*(1), 3–19. https://doi.org/10.1016/S0167-8760(00)00127-6.

Robbins, T. W., Ersche, K. D., & Everitt, B. J. (2008). Drug addiction and the memory systems of the brain. *Annals of the New York Academy of Sciences*, *1141*(1), 1–21. https://doi.org/10.1196/annals.1441.020.

Scheeringa, R., Bastiaansen, M. C., Petersson, K. M., Oostenveld, R., Norris, D. G., & Hagoort, P. (2008). Frontal theta EEG activity correlates negatively with the default mode network in resting state. *International Journal of Psychophysiology*, *67*(3), 242–251. https://doi.org/10.1016/j.ijpsycho.2007.05.017.

Schoenbaum, G., Roesch, M. R., & Stalnaker, T. A. (2006). Orbitofrontal cortex, decision-making and drug addiction. *Trends in Neurosciences*, *29*(2), 116–124. https://doi.org/10.1016/j.tins.2005.12.006.

Semlitsch, H. V., Anderer, P., Schuster, P., & Presslich, O. (1986). A solution for reliable and valid reduction of ocular artifacts,

applied to the P300 ERP. *Psychophysiology*, *23*(6), 695–703. https://doi.org/10.1111/j.1469-8986.1986.tb00696.x.

Soltani, M., & Knight, R. T. (2000). Neural origins of the P300. *Critical Reviews*^{TM} in *Neurobiology*, *14*(3–4). https://doi.org/10.1615/CritRevNeurobiol.v14.i3-4.20.

Sun, Y., Ying, H., Seetohul, R. M., Xuemei, W., Ya, Z., Qian, L., … Ye, S. (2012). Brain fMRI study of crave induced by cue pictures in online game addicts (male adolescents). *Behavioural Brain Research*, *233*(2), 563–576. https://doi.org/10.1016/j.bbr.2012.05.005.

Utevsky, A. V., Smith, D. V., & Huettel, S. A. (2014). Precuneus is a functional core of the default-mode network. *The Journal of Neuroscience*, *34*(3), 932–940. https://doi.org/10.1523/JNEUROSCI.4227-13.2014.

Volkow, N. D., & Fowler, J. S. (2000). Addiction, a disease of compulsion and drive: Involvement of the orbitofrontal cortex. *Cereb Cortex*, *10*(3), 318–325. https://doi.org/10.1093/cercor/10.3.318.

Volkow, N. D., Wang, G. J., Fowler, J. S., Tomasi, D., Telang, F., & Baler, R. (2010). Addiction: Decreased reward sensitivity and increased expectation sensitivity conspire to overwhelm the brain's control circuit. *Bioessays*, *32*(9), 748–755. https://doi.org/10.1002/bies.201000042.

Volpe, U., Mucci, A., Bucci, P., Merlotti, E., Galderisi, S., & Maj, M. (2007). The cortical generators of P3a and P3b: A LORETA study. *Brain Research Bulletin*, *73*(4–6), 220–230. https://doi.org/10.1016/j.brainresbull.2007.03.003.

Wang, Y., Yin, Y., Sun, Y. W., Zhou, Y., Chen, X., Ding, W. N., … Du, Y. S. (2015). Decreased prefrontal lobe interhemispheric functional connectivity in adolescents with internet gaming disorder: A primary study using resting-state FMRI. *Plos One*, *10*(3), e0118733. https://doi.org/10.1371/journal.pone.0118733.

Weiss, F., Maldonado-Vlaar, C. S., Parsons, L. H., Kerr, T. M., Smith, D. L., & Ben-Shahar, O. (2000). Control of cocaine-seeking behavior by drug-associated stimuli in rats: Effects on recovery of extinguished operant-responding and extracellular dopamine levels in amygdala and nucleus accumbens. *Proceedings of the National Academy of Sciences of the United States of America*, *97*(8), 4321–4326. https://doi.org/10.1073/pnas.97.8.4321.

Weng, C. B., Qian, R. B., Fu, X. M., Lin, B., Han, X. P., Niu, C. S., & Wang, Y. H. (2013). Gray matter and white matter abnormalities in online game addiction. *European Journal of Radiology*, *82*(8), 1308–1312. https://doi.org/10.1016/j.ejrad.2013.01.031.

Yoon, E. J., Choi, J. S., Kim, H., Sohn, B. K., Jung, H. Y., Lee, J. Y., … Kim, Y. K. (2017). Altered hippocampal volume and functional connectivity in males with Internet gaming disorder comparing to those with alcohol use disorder. *Scientific Reports*, *7*(1), 5744. https://doi.org/10.1038/s41598-017-06057-7.

Young, K. S. (1996). Psychology of computer use: XL. Addictive use of the internet: A case that breaks the stereotype. *Psychological Reports*, *79*(3), 899–902. https://doi.org/10.2466/pr0.1996.79.3.899.

Yu-Feng, Z., Yong, H., Chao-Zhe, Z., Qing-Jiu, C., Man-Qiu, S., Meng, L., … Yu-Feng, W. (2007). Altered baseline brain activity in children with ADHD revealed by resting-state functional MRI. *Brain & Development*, *29*(2), 83–91. https://doi.org/10.1016/j.braindev.2006.07.002

Yuan, K., Cheng, P., Dong, T., Bi, Y., Xing, L., Yu, D., … Tian, J. (2013). Cortical thickness abnormalities in late adolescence with online gaming addiction. *Plos One*, *8*(1), e53055. https://doi.org/10.1371/journal.pone.0053055.

Yuan, K., Jin, C., Cheng, P., Yang, X., Dong, T., Bi, Y., … Tian, J. (2013). Amplitude of low frequency fluctuation abnormalities in adolescents with online gaming addiction. *Plos One*, *8*(11), e78708. https://doi.org/10.1371/journal.pone.0078708.

Zang, Y., Jiang, T., Lu, Y., He, Y., & Tian, L. (2004). Regional homogeneity approach to fMRI data analysis. *Neuroimage*, *22*(1), 394–400. https://doi.org/10.1016/j.neuroimage.2003.12.030.

Zou, Q. H., Zhu, C. Z., Yang, Y., Zuo, X. N., Long, X. Y., Cao, Q. J., … Zang, Y. F. (2008). An improved approach to detection of amplitude of low-frequency fluctuation (ALFF) for resting-state fMRI: Fractional ALFF. *Journal of Neuroscience Methods*, *172*(1), 137–141. https://doi.org/10.1016/j.jneumeth.2008.04.012.